Proceedings of the ASME 2015 Dynamic Systems and Control Conference
DSCC2015
October 28-30, 2015, Columbus, Ohio, USA

DSCC2015-9825

ADAPTIVE ROBUST CASCADE FORCE CONTROL OF 1-DOF JOINT EXOSKELETON FOR HUMAN PERFORMANCE AUGMENTATION

Shan Chen
The State Key Lab of Fluid Power Transmission and Control (SKLoFPTC)
Zhejiang University
Hangzhou, 310027, China
Emails: chenshan856@126.com

Bin Yao*
SKLoFPTC
Zhejiang University
Hangzhou, 310027, China
School of Mechanical Engineering
Purdue University
West Lafayette, IN47907, USA
Email: byao@purdue.edu

Zheng Chen†
Ocean College
Zhejiang University
Hangzhou, 310027, China
Email: zheng_chen@zju.edu.cn

Xiaocong Zhu
SKLoFPTC
Zhejiang University
Hangzhou, 310027, China
Email: zhuxiaoc@zju.edu.cn

Shiqiang Zhu
Research Center of Robot
Zhejiang University
Hangzhou, 310027, China
Email: sqzhu@zju.edu.cn

ABSTRACT

The control objective of exoskeleton for human performance augmentation is to minimize the human machine interaction force while carrying external loads and following human motion. This paper addresses the dynamics and the interaction force control of a 1-DOF hydraulically actuated joint exoskeleton. A spring with unknown stiffness is used to model the human-machine interface. A cascade force control method is adopted with high-level controller generating the reference position command while low level controller doing motion tracking. Adaptive robust control(ARC) algorithm is developed for both two controllers to deal with the effect of parametric uncertainties and uncertain nonlinearities of the system. The proposed adaptive robust cascade force controller can achieve small human-machine interaction force and good robust performance to model uncertainty which have been validated by experiment.

INTRODUCTION

Exoskeleton for human performance augmentation is a human-machine interaction system which combines the power of the robot with the intelligence of the human. Due to the great potential in reducing the burden for people who carry heavy loads, it has attracted great interest from military and the industry. The development of exoskeleton began in the early 1960s and has experienced great progress in 21th century [1, 2]. The Berkeley Lower Extremity Exoskeleton(BLEEK) [3], Raytheon/Sarcos exoskeleton(XOS) [4]and the HAL exoskeleton [5–7] are typical examples. Exoskeleton robots can be classified according to the measurement method of the human-robot interaction: cHRI-based system and pHRI-based system [8]. The cHRI-based system,like HAL, measures the electric signals from the central nervous system to the musculoskeletal system of humans and use them as inputs to the robot controller. While, the pHRI-based

*Address all correspondence to this author.
†Zheng Chen was working at the Department of Mechanical Engineering, Dalhousie University, Halifax, NSB3H4R2, Canada, before May 2015, and starts to work at Ocean College, Zhejiang University, Hangzhou, 310027, China, in July 2015.

system, such as XOS and BLEEK, measures the force or position/velocity changes that are the results of the motions by the human musculoskeletal system and use them as inputs to the robot controller.

The control objective of exoskeleton for human performance augmentation is to minimize the human machine interaction force while carrying external loads and following human motion. HAL used the EMG signal to compute the muscle torque and finally obtain the assistance torque for exoskeleton based on the muscle torque. The unreliability of EMG sensors limits the generalization of this control algorithm. BLEEK adopted sensitivity amplification control(SAC) in which a positive feedback controller using the inverse dynamics of the plant is used to increase the sensitivity to the force from the human. However, robust performance cannot be guaranteed due to the impossibility of obtaining an accurate inverse dynamics. The XOS system used human-machine interaction force as input of the robot controller. Unfortunately, few papers can be found on the detail of its control method. As for the human-machine interaction force control, several control algorithms have been proposed in the upper exoskeleton systems, such as admittance control in [9], impedance control in [10], and the human-machine cooperation controller design in [11]. Usually these exoskeleton controllers adopt a cascade control method in which the control system is grouped into two levels. High-level controller receives interaction force and produces reference commands(such as position, acceleration or force) while the low level controller is to track the reference from the high-level controller.

It is observed that although there has been significant progress in the development of exoskeleton for human performance augmentation, a number of challenging issues still remain in the precise control of exoskeletons. First, the properties of hydraulic actuator(like significant oil compressibility, leakage) should be considered in the low-level controller design. Also, model uncertainties both from actuator and human-machine interface should be dealt with explicitly for good robust performance. Finally, the hardware physical constraint, low accuracy of the encoders in our system, should be considered when designing control algorithm. If the control algorithm requires velocity or even acceleration feedback, the system cannot be be implemented properly.

In this paper, the modeling and cascade interaction force control of a 1-DOF hydraulically actuated joint exoskeleton is proposed. Springs with unknown stiffness are used to model the human-machine interaction. A simplified first order model for the hydraulic actuator is proposed which makes the low-level controller design simple. In the cascade interaction force control, the low-level controller is chosen to be a trajectory tracking controller since the force tracking of the cylinder is hard to achieved due to the oil leakage. The reference trajectory which can also be considered as human intent, is obtained form the high-level controller by making the integral of the human-machine interaction force become zero. The ARC control methodology is employed in both controllers to deal with the effect of parametric uncertainties and uncertain nonlinearities of the system. In order to guarantee the stability and performance of the whole system, a low-pass filter is used to describe the interaction effect between two subsystems. Comparative experiment verifies that the proposed adaptive robust cascade force control can minimize the human-machine interaction force and good robust performance to load change can be achieved.

MODELING OF THE 1-DOF JOINT SYSTEM

Full-Order Model

The whole hydraulically actuated lower extremity is shown in Fig. 1. This paper only addresses the control problem of the knee joint exoskeleton. It includes three parts, as shown in Fig. 2, the human-machine interface due to the physical contact between the human and the machine, the mechanic system of 1-DOF joint(including the load), and the electro-hydraulic actuator.

FIGURE 1. An exoskeleton system with electro-hydraulic actuation.

For simplicity, a spring is used to model the the human-machine interface and the stiffness of the spring is assumed unknown. The dynamics of the valve is neglected and the control input is assumed to be the displacement of the valve. The whole system is described by Eq.1, which includes the human-machine

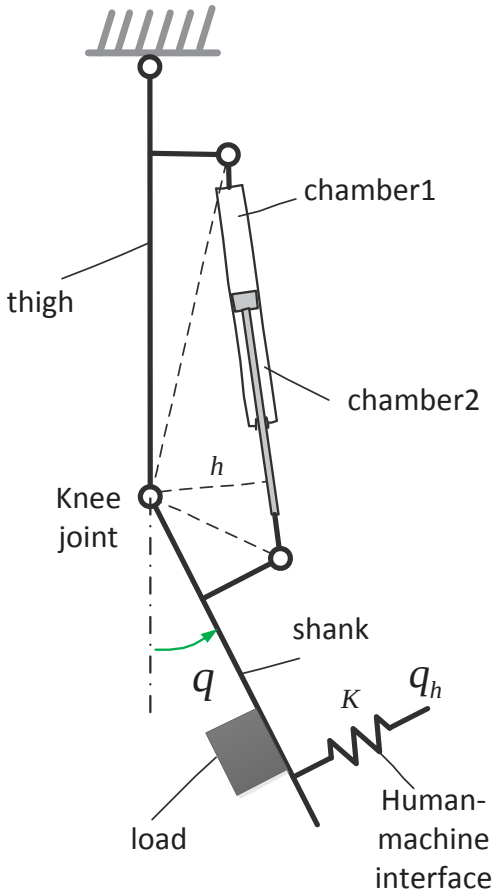

FIGURE 2. A schematic of 1-DOF exoskeleton system.

interaction dynamics, motion dynamics of the cylinder, the pressure dynamics of two hydraulic chambers, and flow rates of the servo valve.

$$\begin{aligned}
T_{hm} &= K(q_h - q) + \tilde{D}_1 \\
J\ddot{q} &= -h(P_1A_1 - P_2A_2) - mgl_c \sin q - B\dot{q} - A \cdot S(\dot{q}) \\
&\quad + T_{hm} + \tilde{D}_2 \\
\tfrac{V_1}{\beta_e}\dot{P}_1 &= A_1 h\dot{q} + Q_1 + \tilde{D}_{31} \\
\tfrac{V_2}{\beta_e}\dot{P}_2 &= -A_2 h\dot{q} - Q_2 + \tilde{D}_{32} \\
Q_1 &= k_{q1}x_v\sqrt{|\Delta P_1|},\ \Delta P_1 = \begin{cases} P_s - P_1 \ if\ x_v \geq 0 \\ P_2 - P_r \ if\ x_v < 0 \end{cases} \\
Q_2 &= k_{q2}x_v\sqrt{|\Delta P_2|},\ \Delta P_2 = \begin{cases} P_2 - P_r \ if\ x_v \geq 0 \\ P_s - P_2 \ if\ x_v < 0 \end{cases} \\
x_v &= u
\end{aligned} \tag{1}$$

where T_{hm} is human-machine interaction force; K is the stiffness of the human-machine interface; q_h and q are the positions of human and the machine, respectively; $\tilde{D}_1$ is the lumped uncertainties and disturbances at the human-machine interface; J is the moment of inertia of the robotic shank and external payload lumped together; h is the moment arm of the output force of hydraulic cylinder; P_1 and P_2 are the absolute pressures of chamber 1 and chamber 2; A_1 and A_2 are the acting areas of two chambers, respectively; m is the total load mass; l_c is the distance between the joint and the contact point; B is the combined coefficients of the damping and viscous friction, A is the unknown Coulomb friction coefficient and $S(\dot{q})$ is a known continuous function used to approximate the traditional discontinuous sign function $sgn(\dot{q})$ for effective friction compensation in implementation, $S(\dot{q}) = \frac{2}{\pi}\arctan(900\dot{q})$, $\tilde{D}_2$ is the lumped uncertainties and disturbances acting on the joint exoskeleton; V_1, V_2 are volumes of two chambers, $V_1 = V_{h1} - h\dot{q}$, $V_2 = V_{h2} + h\dot{q}$; V_{h1}, V_{h2} are two chamber volumes when $q = 0$; β_e is effective bulk modulus, Q_1, Q_2 are the supply flow and return flow,respectively; $\tilde{D}_{31}$,$\tilde{D}_{32}$ are the lumped modeling error and uncertainties in the forward and return loop respectively; x_v is the spool displacement, k_{q1} and k_{q2} are the flow gain coefficients for the forward and return loop, respectively, P_s is the supply pressure of the pump and P_r is the reference pressure in the return tank; u is the control voltage for the valve.

Since the relationship among T_{hm}, q_h and q is static, in order to dynamically control the interaction force, the integral of interaction force is controlled instead of the pure interaction force in the controller design [12]. Finally, the problem addressed in this paper is the construction of a control law $u(t)$ that causes the integral of human-machine interaction force $\int_0^t T_{hm}$ to go to zero quickly and exactly.

Let $x = \left[\int_0^t T_{hm}\ q\ \dot{q}\ P_1\ P_2\right]^T$, $\tilde{\Delta}_1 = Kq_h + \tilde{D}_1$, $\tilde{\Delta}_3 = \frac{1}{J}\tilde{D}_2$, $\tilde{\Delta}_4 = \tilde{D}_{31}\beta_e\frac{A_1}{V_1} + \tilde{D}_{32}\beta_e\frac{A_2}{V_2}$. Separating the lumped uncertainties into constant part and the time-varying part $\tilde{\Delta}_i = \Delta_{in} + \Delta_i, i = 1,3,4$. Let $\theta = \left[K\ \Delta_{1n}\ \frac{1}{J}\ \frac{mgl_c}{J}\ \frac{B}{J}\ \frac{A}{J}\ \Delta_{3n}\ \beta_e\ \Delta_{4n}\right]^T$. The entire system can be expressed as

$$\begin{aligned}
\dot{x}_1 &= -\theta_1 x_2 + \theta_2 + \Delta_1 \\
\dot{x}_2 &= x_3 \\
\dot{x}_3 &= -\theta_3 h(A_1x_4 - A_2x_5) - \theta_4 \sin x_2 - \theta_5 x_3 \\
&\quad -\theta_6 \cdot S(x_3) + \theta_8 + \Delta_3 \\
A_1\dot{x}_4 - A_2\dot{x}_5 &= \theta_8\left(Q_1\tfrac{A_1}{V_1} + Q_2\tfrac{A_2}{V_2}\right) + \theta_8\left(\tfrac{A_1^2}{V_1}h + \tfrac{A_2^2}{V_2}h\right)x_3 \\
&\quad +\theta_9 + \Delta_4
\end{aligned} \tag{2}$$

Reduced-Order Model

For the full-order model as shown in Eq. 2, by differentiating the dynamics of $\dot{x}_3$ and substituting the dynamics equation of $\dot{x}_4$,$\dot{x}_5$, the last two dynamics of Eq. 2 become as

$$\begin{aligned}
&\dddot{x}_3 + \theta_5\ddot{x}_3 + \left(\theta_3 h\theta_8\left(\tfrac{A_1^2}{V_1}h + \tfrac{A_2^2}{V_2}h\right) + \theta_4\cos x_2\right)\dot{x}_3 \\
&= -\theta_3 h\theta_8\left(Q_1\tfrac{A_1}{V_1} + Q_2\tfrac{A_2}{V_2}\right) + \dot{\tilde{\Delta}}_e
\end{aligned} \tag{3}$$

where $\tilde{\Delta}_e = -\theta_6 \cdot \dot{S}(x_3) + \dot{\Delta}_3 - \theta_3 h \dot{\Delta}_4$ which is the equivalent disturbance.

The natural frequency of this second order system is

$$\omega_n = \sqrt{\theta_3 h \theta_8 \left(\frac{A_1^2}{V_1} h + \frac{A_2^2}{V_2} h\right) + \theta_4 \cos x_2} \tag{4}$$

Often θ_9 is very large in the level of 10^8, and V_1, V_2 mainly depend on the volume of pipes and change little. If θ_3 is also large which means the inertial is small, and the moment arm h is large, then ω_n has a large value. Therefore the dynamics shown in Eq. 3 can be neglected and the steady-state relationship becomes

$$\begin{aligned} &\left(\theta_3 h \theta_8 \left(\frac{A_1^2}{V_1} h + \frac{A_2^2}{V_2} h\right) + \theta_4 \cos x_2\right) x_3 \\ &= -\theta_3 h \theta_8 \left(Q_1 \frac{A_1}{V_1} + Q_2 \frac{A_2}{V_2}\right) + \theta_e + \Delta_e \end{aligned} \tag{5}$$

where θ_e and Δ_e are the constant part and time-varying part of the lumped distrubance $\tilde{\Delta}_e$, which means $\tilde{\Delta}_e = \theta_e + \Delta_e$.

Finally, the reduced-order dynamics of the whole human-machine system is with order of two and the state-space representation becomes

$$\begin{aligned} \dot{x}_1 &= -\theta_1 x_2 + \theta_2 + \Delta_1 \\ \dot{x}_2 &= \sigma(x_2)\left(Q_1 \frac{A_1}{V_1} + Q_2 \frac{A_2}{V_2}\right) + \varphi_2(x_2)\theta_e + \Delta_{e2} \end{aligned} \tag{6}$$

where $\sigma(x_2) = -\frac{\theta_3 h \theta_8}{\theta_3 h \theta_8 \left(\frac{A_1^2}{V_1} h + \frac{A_2^2}{V_2} h\right) + \theta_4 \cos x_2}$, $\varphi_2(x_2) = \frac{1}{\theta_3 h \theta_8 \left(\frac{A_1^2}{V_1} h + \frac{A_2^2}{V_2} h\right) + \theta_4 \cos x_2}$, $\Delta_{e2} = \frac{1}{\theta_3 h \theta_8 \left(\frac{A_1^2}{V_1} h + \frac{A_2^2}{V_2} h\right) + \theta_4 \cos x_2} \Delta_e$.

The following nomenclature is used throughout this paper: $\hat{\bullet}$ is used to denote the estimate of $\bullet$, $\tilde{\bullet}$ is used to denote the estimation error of $\bullet$, e.g., $\tilde{\theta} = \hat{\theta} - \theta$, $\bullet_i$ is the ith component of the vector $\bullet$, $\bullet_{max}$, and $\bullet_{min}$ are the maximum and minimum value of $\bullet(t)$ for all t , respectively.

ADAPTIVE ROBUST CASCADE FORCE CONTROL

The controller design is based on cascade control strategy in which the high-level force controller receives interaction force and produces trajectory reference while the low level motion controller makes the exoskeleton joint track the trajectory reference from the high-level controller. It is assumed that only $\theta_1, \theta_2, \theta_e$ to be unknown parameters. The design procedure is as follows.

High-level Force Controller Design

The high-level force controller is designed based on the following dynamics

$$\dot{x}_1 = -\theta_1 x_2 + \theta_2 + \Delta_1 \tag{7}$$

Let

$$z_1 = x_1 - x_{1d} \tag{8}$$

where x_{1d} is the integral of desired human-machine interaction force trajectory and can be set to be any small values(x_{1d} is set to be zero in the following experiment).

The problem addressed in this stage is the construction of a control law $x_2(t)$ that causes the interaction force tracking error z_1 to go to zero quickly and exactly. Let $\beta = \begin{bmatrix} \theta_1 & \theta_2 \end{bmatrix}^T$. Differentiating Eq.8 and substituting Eq.7 into it, one obtains

$$\dot{z}_1 = -\theta_1 x_2 + \theta_2 + \Delta_1 - \dot{x}_{1d} \tag{9}$$

Design a control law α_1 for x_2 as follows:

$$\begin{aligned} &\alpha_1 = \alpha_{1a} + \alpha_{1s1} + \alpha_{1s2} \\ &\alpha_{1a} = -\tfrac{1}{\hat{\theta}_1}\left(\dot{x}_{1d} - \hat{\theta}_2\right) \\ &\alpha_{1s1} = -\tfrac{1}{\hat{\theta}_{1\min}}\left(-k_{1s1} z_1\right), \qquad k_{1s1} = g_1 \|\Gamma_1 \phi_1\|^2 + k_1 \end{aligned} \tag{10}$$

where $k_1 > 0$, $g_1 \geq 0$, $\Gamma_1 > 0$ is a diagonal adaptation rate matrix. $\phi_1 = \begin{bmatrix} -\alpha_{1a} & 1 \end{bmatrix}^T$.

Let $\bar{\Delta}_1 = \Delta_1$, $\tau_1 = \omega_1 \phi_1 z_1$ where ω_1 is a positive weighting factor, α_{1s2} is chosen to satisfy the following two conditions

$$\begin{aligned} &z_1\left(-{\phi_1}^T \tilde{\beta} + \bar{\Delta}_1 + (-\theta_1 \alpha_{1s2})\right) \leq \varepsilon_1 \\ &-\theta_1 z_1 \alpha_{1s2} \leq 0 \end{aligned} \tag{11}$$

where ε_1 is a positive design parameter which can be arbitrarily small. Then the error subsystem becomes

$$\dot{z}_1 + \frac{\theta_1}{\hat{\theta}_{1\min}} k_{1s1} z_1 = -{\phi_1}^T \tilde{\beta} + \bar{\Delta}_1 + (-\theta_1 \alpha_{1s2}) \tag{12}$$

Choose $V_{s1} = \frac{1}{2}\omega_1 z_1^2$. Its time derivative becomes

$$\dot{V}_{s1} = -\omega_1 \frac{\theta_1}{\hat{\theta}_{1\min}} k_{1s1} z_1^2 + \omega_1 z_1 \left(\bar{\Delta}_1 - \theta_1 \alpha_{1s2}\right) - \tilde{\beta}^T \tau_1 \tag{13}$$

The adaptation law is chosen to be

$$\dot{\hat{\beta}} = Proj(\Gamma_1 \tau_1) \tag{14}$$

Low-level Motion Controller design

The low-level motion controller is designed based on the following dynamics

$$\dot{x}_2 = \sigma(x_2)\left(Q_1\frac{A_1}{V_1} + Q_2\frac{A_2}{V_2}\right) + \varphi_2(x_2)\theta_e + \tilde{\Delta}_{e2} \tag{15}$$

Let

$$z_2 = x_2 - x_{2d} \tag{16}$$

where x_{2d} is the desired trajectory that x_2 want to track. For the exoskeleton system, x_{2d} is obtained by passing the control input α_1 designed in high level loop through a low pass filter.

The problem addressed in this stage is the construction of a control law $u(t)$ that causes the trajectory tracking error z_2 to go to zero quickly and exactly. Differentiating Eq.16 and substituting Eq.15 into it, one obtains

$$\dot{z}_2 = \sigma(x_2)Q_L + \varphi_2(x_2)\theta_e + \tilde{\Delta}_{e2} - \dot{x}_{2d} \tag{17}$$

where $Q_L = Q_1\frac{A_1}{V_1} + Q_2\frac{A_2}{V_2}$.

Design a control law α_2 for Q_L as follows:

$$\begin{array}{l} \alpha_2 = \alpha_{2a} + \alpha_{2s1} + \alpha_{2s2} \\ \alpha_{2a} = \frac{1}{\sigma(x_2)}(\dot{x}_{2d} - \varphi_2(x_2)\hat{\theta}_e) \\ \alpha_{2s1} = \frac{1}{\sigma(x_2)}(-k_{2s1}z_2) \\ k_{2s1} = g_2\|\Gamma_2\phi_2\|^2 + k_2 \end{array} \tag{18}$$

where $k_2 > 0$, $g_2 \geq 0$, $\Gamma_2 > 0$ is a diagonal adaptation rate matrix, $\phi_2 = \varphi_2(x_2)$.

Let $\bar{\Delta}_2 = \tilde{\Delta}_{e2}$, $\tau_2 = \omega_2\phi_2 z_2$ where ω_2 is a positive weighting factor, α_{2s2} is chosen to satisfy the following two conditions

$$\begin{array}{l} z_2\left(-{\phi_2}^T\tilde{\theta}_e + \bar{\Delta}_2 + \sigma(x_2)\alpha_{2s2}\right) \leq \varepsilon_2 \\ z_2\sigma(x_2)\alpha_{2s2} \leq 0 \end{array} \tag{19}$$

where ε_2 is a positive design parameter which can be arbitrarily small. Then the error subsystem becomes:

$$\dot{z}_2 = -k_{2s1}z_2 + \left(-{\phi_2}^T\tilde{\theta}_e + \bar{\Delta}_2 + \sigma(x_2)\alpha_{2s2}\right) \tag{20}$$

Choose $V_{s2} = \frac{1}{2}\omega_2 z_2^2$. Its time derivative becomes

$$\begin{array}{l} \dot{V}_{s2} = \omega_2\left(-k_{2s1}z_2^2 + z_2\left(-{\phi_2}^T\tilde{\theta}_e + \bar{\Delta}_2 + \sigma(x_2)Q_{Ls2}\right)\right) \\ -\tilde{\theta}_e^T\tau_2 \end{array} \tag{21}$$

Finally, the control input $u(t)$ can be solved from the following:

$$u = \frac{\alpha_2}{\frac{A_1}{V_1}k_{q1}\sqrt{|\Delta P_1|} + \frac{A_2}{V_2}k_{q2}\sqrt{|\Delta P_2|}} \tag{22}$$

The adaptation law is chosen to be:

$$\dot{\hat{\theta}}_e = Proj(\Gamma_2\tau_2) \tag{23}$$

Main Results

The ARC control law Eq.10 and Eq.22 guarantee the following

A. In general, for each local closed loop system (low-level loop and high-level loop), all signals are bounded. Furthermore, V_{s1}, V_{s2} are bounded above by

$$\begin{array}{l} V_{s1}(t) \leq \exp(-\lambda_1 t)V_{s1}(0) + \frac{\varepsilon_1}{\lambda_1}[1-\exp(-\lambda_1 t)] \\ V_{s2}(t) \leq \exp(-\lambda_2 t)V_{s2}(0) + \frac{\varepsilon_2}{\lambda_2}[1-\exp(-\lambda_2 t)] \end{array} \tag{24}$$

where $\lambda_1 = 2\frac{\theta_1}{\theta_{1\min}}k_1$, $\lambda_2 = 2k_2$.

B. For each local closed loop system, if after a finite time t_0, $\Delta_1 = 0$, $\Delta_{e2} = 0$, $\forall t \geq t_0$, i.e., in the presence of parametric uncertainties only, then, in addition to results in A, asymptotic output tracking (or zero final tracking error) is achieved, i.e.,$z_1 \to 0$, $z_2 \to 0$, as $t \to \infty$.

Following the standard discontinuous projection-based ARC arguments as in [13–15], the theorem can be proved.

The theory results achieved above can only guarantee the stability and performance of each independent local closed loop system. If we want the whole closed loop system to work effectively, the closed loop bandwidth of the high-level loop cannot be chosen too large since the high level controller design is based on the hypothesis that the low-level closed loop system is fast enough.

The reference trajectory for low level motion controller is generated by passing α_1 computed from high-level controller to a low pass filter with order no less than two. It has two functions:1) Generate the desired velocity which is needed in the low level controller design. 2) In some level, consider the interaction effect between the two closed loop subsystems, which is useful in increasing the bandwidth of the high level controller.

COMPARATIVE EXPERIMENT

To illustrate the above design, experiment results are obtained for a 1-DOF joint exoskeleton having the following parameters: $P_s = 4.6Mpa$, $P_r = 0.05Mpa$, $A_1 = 3.142e-4m^2$, $A_2 =$

$1.131e-4m^2$, $V_{h1} = 9.896e-5m^3$, $V_{h2} = 2.0595e-5m^3$. Sampling time is $t_s = 10ms$. A force sensor is mounted in the joint exoskeleton to measure the human-machine interaction force. An encoder is mounted in the knee joint to measure the joint position. Backward difference plus filter is used to obtain the velocity information. Human manipulate the joint by pulling and pressing the force sensor by hand. For simplicity, the needed robust control terms α_{1s2} and α_{2s2} are implemented by simply choose the linear feedback gain large enough. The off-line estimate of θ is $\hat{\theta}(0) = \begin{bmatrix} 1 & 0 & 3.4 & 20.7 & 1.5 & 0.164 & 0 & 8.7e7 & 0 \end{bmatrix}^T$, $\hat{\theta}_e(0) = 0$.

For the low-level motion controller, the following three controllers are compared:

C1: PID control with velocity feedforward. The control law is

$$u = k_p z_2 - VF\dot{x}_{2d} \tag{25}$$

where kp=30, VF=0.6.

C2: Deterministic robust control in low-level controller design but without using parameter adaptation. The control gains are chosen as $k_2 = 30$, $\omega_2 = 1$. The adaptation rate is set as $\Gamma_2 = 0$.

C3: The adaptive robust motion controller in low-level controller design. The control gains are chosen as $k_2 = 30$, $\omega_2 = 1$. The adaptation rates is set as $\Gamma_2 = 2e3$.

For the high-level force controller, the following two controllers are compared:

FDRC: Deterministic robust force control in high level controller design without using parameter adaptation. The control gains are chosen as $k_1 = 20$, $\omega_1 = 1$. The adaptation rate is set as $\Gamma_1 = \begin{bmatrix} 0 & 0 \end{bmatrix}$.

FARC: Adaptive robust force control in high level controller design. The control gains are chosen as $k_1 = 20$, $\omega_1 = 1$. The adaptation rate is set as $\Gamma_1 = \begin{bmatrix} 0 & 60 \end{bmatrix}$.

The control schemes are applied to the following test sets:

Set1: To test the trajectory tracking performance of the low-level controllers. The reference is chosen to be a point to point trajectory with maximum velocity of $0.1rad/s$ and maximum acceleration of $0.3rad/s^2$.

Set2: To test the interaction force control performance of the high-level controllers. The low level controller is fixed and chosen to be C1.

Set3: To test the interaction force control performance with different low level controllers. The high level controller is fixed and chosen to be FARC.

Set4: To test the robust performance of cascade force controllers to parameter variations, a 1.72 kg payload is mounted on the knee joint.

The trajectory tracking error for Set1 is shown in Fig.3. It can be seen that the trajectory tracking performance of ARC and DRC are much better than PID. Also, due to parameter adaptation as shown in Fig.4, ARC can achieve a smaller tracking error than DRC.

TABLE 1. NORMALIZED AVERAGE INTERACTION FORCE

	$\|F_{hm}\|_{nrms}$
FDRC+C1(Set2)	0.1954
FARC+C1(Set2)	0.1370
FARC+C2(Set3)	0.1345
FARC+C3(Set3)	0.1231
FARC+C1(Set4)	0.1381
FARC+C2(Set4)	0.1261
FARC+C3(Set4)	0.1253

Since it is impossible for the human to manipulate the exoskeleton with identical velocity across individual experiments, we do the normalization of interaction force when demonstrating the comparative experiment results. Define the performance index: normalized average interaction force ($\|F_{hm}\|_{nrms} = (\frac{1}{T}\int_0^T |F_{hm}|^2 dt)^{1/2} / (\frac{1}{T}\int_0^T |\dot{q}|^2 dt)^{1/2}$). Experimental results in terms of the normalized average interaction force are given in table1.

The human-machine interaction force and velocity of the joint exoskeleton for Set2 are shown in Fig.5-Fig.6. The parameter estimate of lumped modeling error of human-machine interface(θ_2) for FARC is shown in Fig.7. In terms of normalized interaction force in Set2, FARC can achieve smaller interaction force than FDRC which demonstrate the effectiveness of parameter adaptation in high-level controller.

When testing the interaction force control performance with different low level controllers in Set3 and Set4, from Fig.8-Fig.9 and table.1, it can be seen that the proposed adaptive robust cascade force controller(FARC+C3) can achieve a small interaction force and consistent performance to load change. However, little performance difference exist for various low level motion controllers. The reason is that the ARC force controller in the high level loop has achieved a good performance that only small model uncertainties left in the low level loop. Also, due to the low accuracy of the encoder, the closed loop bandwidth achieved in low level loop is not large(about $20rad/s$). Small model uncertainties and closed loop bandwidth lead to the almost same motion tracking performance for various low level motion controllers. A more evident comparative result can be achieved if the closed loop bandwidth of the system can be increased. We will improve the experiment results in future work.

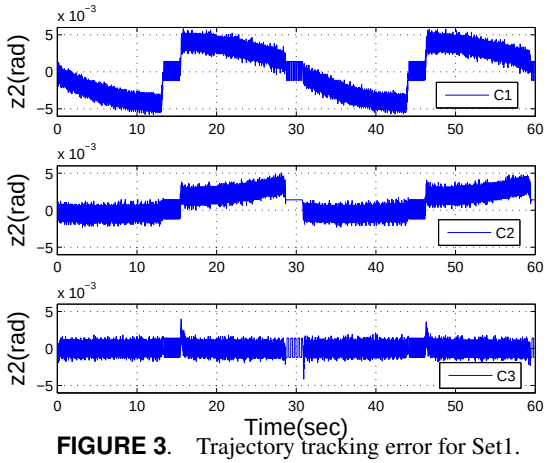

FIGURE 3. Trajectory tracking error for Set1.

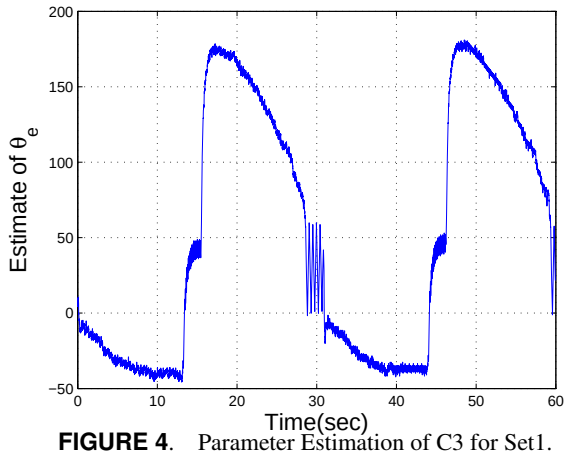

FIGURE 4. Parameter Estimation of C3 for Set1.

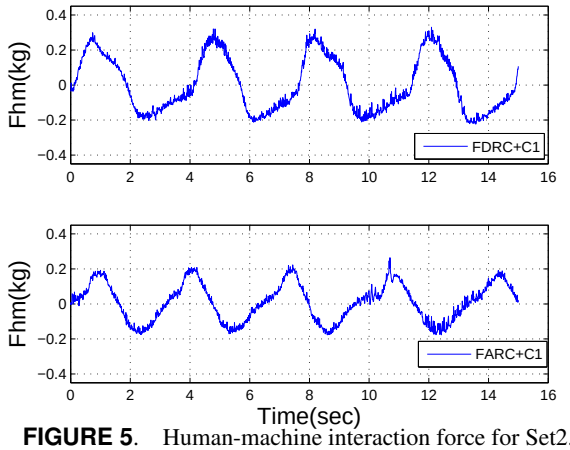

FIGURE 5. Human-machine interaction force for Set2.

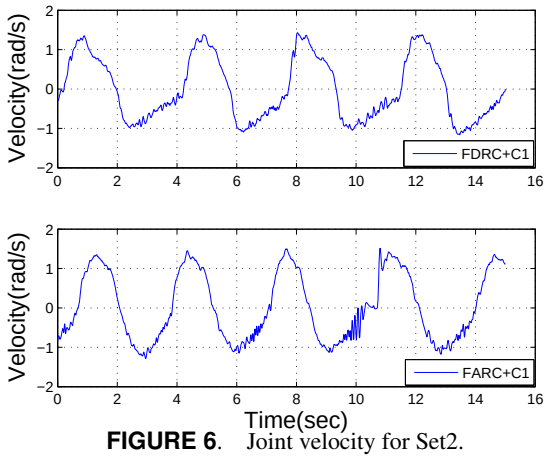

FIGURE 6. Joint velocity for Set2.

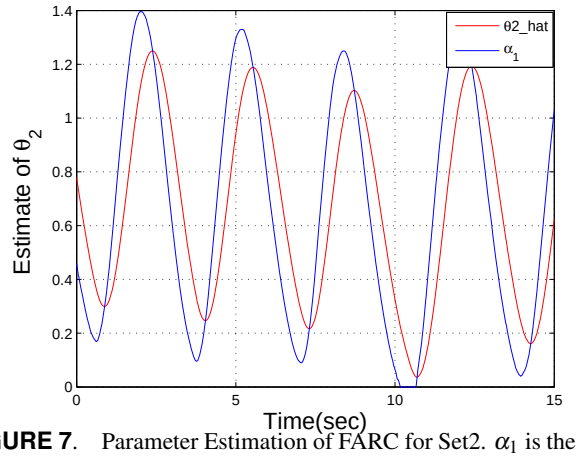

FIGURE 7. Parameter Estimation of FARC for Set2. α_1 is the human intent computed from high level controller.

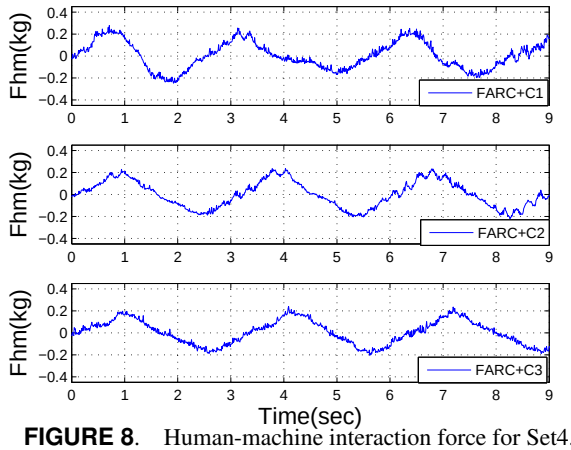

FIGURE 8. Human-machine interaction force for Set4.

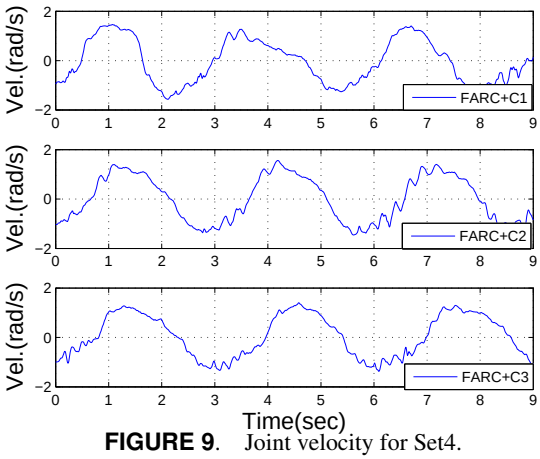

FIGURE 9. Joint velocity for Set4.

CONCLUSIONS

In this paper, a modeling and control of a 1-DOF knee joint exoskeleton aims at minimize the integral of the human machine interaction force for human performance augmentation is proposed. A spring with unknown stiffness is used to model the human-machine interface and a simplified first order system is used to model the hydraulic actuator. A cascade force control method is adopted and adaptive robust control theory has been applied to improve the robustness performance of the system to various model uncertainties. Comparative experiments demonstrated that the proposed adaptive robust cascade force controller can achieve smaller interaction force as well as good robust performance to model uncertainties.

ACKNOWLEDGMENT

This work is supported by National Natural Science Foundation of China (No.51475412 and No.51375432), Science Fund for Creative Research Groups of National Natural Science Foundation of China (No.51221004), the National Basic Research and Development Program of China under 973 Program Grant 2013CB035400 and SANLIAN (SHANGHAI) GROUP (No.H20131864).

REFERENCES

[1] Dollar, A. M., and Herr, H., 2008. "Lower extremity exoskeletons and active orthoses: challenges and state-of-the-art". *Robotics, IEEE Transactions on,* ***24***(1), pp. 144–158.

[2] Kazerooni, H., 2008. "Exoskeletons for human performance augmentation". In *Springer handbook of robotics*. Springer, pp. 773–793.

[3] Zoss, A. B., Kazerooni, H., and Chu, A., 2006. "Biomechanical design of the berkeley lower extremity exoskeleton (bleex)". *Mechatronics, IEEE/ASME Transactions on,* ***11***(2), pp. 128–138.

[4] Guizzo, E., and Goldstein, H., 2005. "The rise of the body bots [robotic exoskeletons]". *Spectrum, IEEE,* ***42***(10), pp. 50–56.

[5] Kasaoka, K., and Sankai, Y., 2001. "Predictive control estimating operator's intention for stepping-up motion by exo-skeleton type power assist system hal". In Intelligent Robots and Systems, 2001 IEEE/RSJ International Conference on, Vol. 3, IEEE, pp. 1578–1583.

[6] Kawamoto, H., Lee, S., Kanbe, S., and Sankai, Y., 2003. "Power assist method for hal-3 using emg-based feedback controller". In Systems, Man and Cybernetics, 2003 IEEE International Conference on, Vol. 2, IEEE, pp. 1648–1653.

[7] Hayashi, T., Kawamoto, H., and Sankai, Y., 2005. "Control method of robot suit hal working as operator's muscle using biological and dynamical information". In Intelligent Robots and Systems, 2005 IEEE/RSJ International Conference on, IEEE, pp. 3063–3068.

[8] Lee, H., Kim, W., Han, J., and Han, C., 2012. "The technical trend of the exoskeleton robot system for human power assistance". *International Journal of Precision Engineering and Manufacturing,* ***13***(8), pp. 1491–1497.

[9] Wen, Y., Jacob, R., and Xiaoou, L., 2011. "Pid admittance control for an upper limb exoskeleton". In American Control Conference, 2011., Vol. 3, IEEE, pp. 1124–1129.

[10] Lee, H., Lee, B., Kim, W., Gil, M., Han, J., and Han, C., 2012. "Human-robot cooperative control based on phri (physical human-robot interaction) of exoskeleton robot for a human upper extremity". *International Journal of Precision Engineering and Manufacturing,* ***13***(6), pp. 985–992.

[11] Lee, H.-D., Lee, B.-K., Kim, W.-S., Han, J.-S., Shin, K.-S., and Han, C.-S., 2014. "Human–robot cooperation control based on a dynamic model of an upper limb exoskeleton for human power amplification". *Mechatronics,* ***24***(2), pp. 168–176.

[12] Yao, B., and Tomizuka, M., 1993. "Adaptive control of robot manipulators in constrained motion". In American Control Conference, 1993, IEEE, pp. 1128–1132.

[13] Yao, B., 1997. "High performance adaptive robust control of nonlinear systems: a general framework and new schemes". In Decision and Control, the 36th IEEE Conference on, Vol. 3, IEEE, pp. 2489–2494.

[14] Yao, B., and Tomizuka, M., 1997. "Adaptive robust control of siso nonlinear systems in a semi-strict feedback form". *Automatica,* ***33***(5), pp. 893–900.

[15] Yao, B., Bu, F., Reedy, J., and Chiu, G.-C., 2000. "Adaptive robust motion control of single-rod hydraulic actuators: theory and experiments". *Mechatronics, IEEE/ASME Transactions on,* ***5***(1), pp. 79–91.